

Paired electrolysis-enabled nickel-catalyzed enantioselective reductive cross-coupling between α -chloroesters and aryl bromides

Received: 28 July 2022

Accepted: 17 November 2022

Published online: 28 November 2022

Check for updates

Dong Liu^{1,3}, Zhao-Ran Liu^{1,3}, Zhen-Hua Wang^{1,3}, Cong Ma¹, Simon Herbert², Hartmut Schirok² & Tian-Sheng Mei¹

Electrochemical asymmetric catalysis has emerged as a sustainable and promising approach to the production of chiral compounds and the utilization of both the anode and cathode as working electrodes would provide a unique approach for organic synthesis. However, precise matching of the rate and electric potential of anodic oxidation and cathodic reduction make such idealized electrolysis difficult to achieve. Herein, asymmetric cross-coupling between α -chloroesters and aryl bromides is probed as a model reaction, wherein alkyl radicals are generated from the α -chloroesters through a sequential oxidative electron transfer process at the anode, while the nickel catalyst is reduced to a lower oxidation state at the cathode. Radical clock studies, cyclic voltammetry analysis, and electron paramagnetic resonance experiments support the synergistic involvement of anodic and cathodic redox events. This electrolytic method provides an alternative avenue for asymmetric catalysis that could find significant utility in organic synthesis.

Asymmetric synthetic electrochemistry has a long history that was long limited by its reliance on ionic additives and a focus on the transfer of electrons from the electrode directly to the organic substrate^{1–5}. Early effort toward asymmetric synthetic electrochemical methods was focused on leveraging chiral solvents, electrolytes, electrodes, mediators, or auxiliaries¹. Later, chiral organocatalysts were introduced as sub-stoichiometric alternatives^{6–11}, and more recently, transition metal catalysis has been applied to electrochemical syntheses of valuable chiral compounds either by anodic oxidation or cathodic reduction^{12–23}. By and large, in these processes, either hydrogen is generated, or a sacrificial anode is employed to ensure electroneutrality (Fig. 1a). Alternatively, paired electrolysis in undivided cells provides a more practical, atom-economical, and energy-efficient approach since both electrodes do work directly necessary for product formation^{24–28}. However, paired electrolysis requires the rate and electric potential of the anodic oxidative reaction and the cathodic reductive reaction to be nearly perfectly matched^{29–39}. Additionally, the heterogeneous electron transfer from the electrode to a substrate makes this process more

challenging^{40,41}. To this end, the merger of asymmetric electrochemical catalysis with paired electrolysis is desired, however, it remains a significant challenge in electrochemical synthesis.

α -Arylated carbonyls are a class of useful scaffolds found widely in natural products and synthetic medicines^{42–44}. Generally, these compounds are synthesized by asymmetric transition metal-catalyzed enolate arylation with the assistance of a strong base^{45–51}. Alternatively, it could be obtained by transition metal-catalyzed enantioselective cross-coupling of α -chloroesters with organometallic reagents^{52–56}. Recently, asymmetric reduction coupling of two electrophiles with chemical reductants to turn over the catalyst allowed the synthesis of α -arylated carbonyls under relatively mild reaction conditions^{57,58}. Walsh and Mao reported a photo-induced nickel-catalyzed asymmetric reductive coupling of α -chloro esters with aryl iodides with Hantzsch ester as the terminal reductant⁵⁷. With their own developed chiral BiOX ligand, Reisman and co-workers demonstrated nickel-catalyzed asymmetric reductive cross-coupling of α -chloroesters and (hetero) aryl iodides with Mn powder as reductant⁵⁸. However, the reductive

¹State Key Laboratory of Organometallic Chemistry, Shanghai Institute of Organic Chemistry, University of Chinese Academy of Sciences, CAS, Shanghai, China. ²Pharmaceuticals, Research and Development, Bayer AG, 13353 Berlin, Germany. ³These authors contributed equally: Dong Liu, Zhao-Ran Liu, Zhen-Hua Wang. e-mail: mei7900@sioc.ac.cn

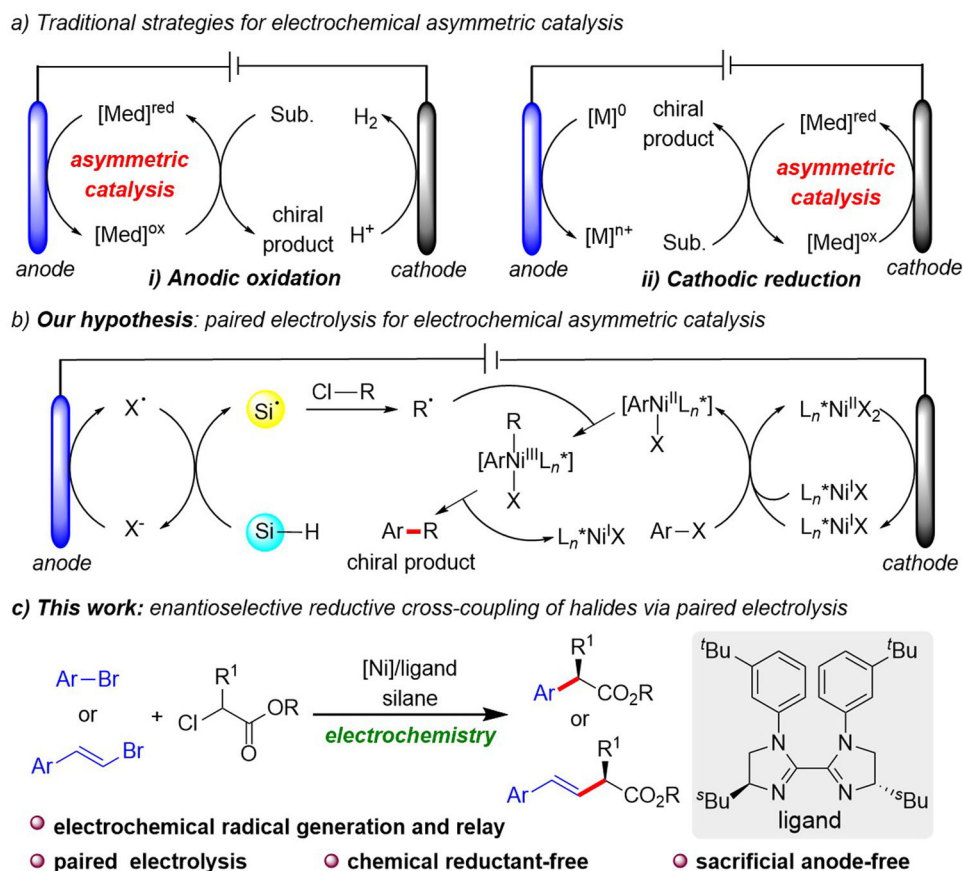


Fig. 1 | Electrochemical asymmetric catalysis. **a** Traditional strategies for electrochemical asymmetric catalysis. **b** Paired electrolysis for electrochemical asymmetric catalysis. **c** This work.

cross-coupling of aryl bromides with α -chloroesters remains a significant challenge, presumably owing to the lower reactivity of aryl bromide with the nickel catalyst compared with aryl iodides^{57,58}.

Pursuant to our interest in synthetic organic electrochemistry^{59,60}, we envisioned that the merger of paired electrolysis and asymmetric nickel catalysis could provide an alternative strategy for catalytic enantioselective reductive couplings of alkyl halides and aryl halides (Fig. 1b). Because of its low oxidation potential compared to the reactants⁶¹, the halide could be preferentially oxidized at the anode to create a halogen radical^{62,63}. Hydrogen atoms from a silane could be rapidly abstracted by the halogen radical to generate a silyl radical, which may subsequently abstract a halogen atom from an alkyl halide and generate an alkyl radical^{64–67}. Simultaneously, cathodic reduction of $[\text{Ni}^{\text{II}}]$ to $[\text{Ni}^{\text{I}}]$ enables oxidative addition of aryl halide to give intermediate $[\text{ArNi}^{\text{III}}\text{X}]$, which traps an alkyl radical to give $[\text{ArNi}^{\text{III}}\text{RX}]$, from which reductive elimination affords an α -arylated cross-coupling product^{68–70}. Herein, we reported the example of paired electrolysis-enabled enantioselective reductive cross-coupling between aryl bromides and α -chloroesters by using a chiral bis-imidazoline (BiIM) ligand (Fig. 1c).

Results

Optimization studies

Initially, the racemic reaction was optimized using methyl 4-bromobenzoate (**1a**), α -chloro ester (**1b**), $\text{NiBr}_2 \cdot \text{glyme}$ (10 mol%), di-*t*-Bubpy (15 mol%), tris(trimethylsilyl)silane (TTMSS) (2.0 equiv), 2,6-lutidine (2.0 equiv), *n*- Bu_4NBF_4 (1.0 equiv) and DMAc (2.0 mL) under constant-current electrolysis at 6.0 mA for 6.0 h at room temperature, giving 90% isolated yield (Table 1, entry 1) (see Supplementary Table 1 for details). Next, we studied electrochemical

asymmetric reactions by investigating various chiral bioxazoline (BiOX) ligands according to previous reports on asymmetric reductive cross-couplings^{57,58}. To our delight, Bn-BiOX (**L1**) could give 44% enantiomeric excess (ee) (entry 2). Further investigation of the BiOX family of ligands (entries 3–6) found that *s*-Bu-BiOX (**L4**) performed best, affording 77% ee with a 25% yield (entry 5). Then, we opted to modify the ester OR group to further improve the enantioselectivity. Unfortunately, replacing the ethyl group with PMP, O^{*i*}Pr, or *t*-Bu groups gave similar results (entries 7–9). Inspired by the work of Nakamura⁷¹, we increased the steric bulk of the ester OR substituent to 2,3,3-trimethylbut-2-yl, affording the desired product in 84% ee (entry 10). In addition, 4-heptyl substituted BiOX ligand (**L6**) gave 89% ee, although the yield was still low (entry 11)^{72,73}. As the structural analog, chiral Bi-imidazoline (BiIM) ligands are also often employed in asymmetric Ni catalysis^{74–84}. Therefore, we changed the sec-butyl and 4-heptyl substituted BiOX to corresponding chiral BiIM ligands (**L7** and **L8**), affording the desired product in 90% ee with 30% yield and 84% ee with 25% yield, respectively (entries 12 and 13). To our delight, under a cell potential of 2.9 V, with 3.0 equivalents of lutidine and 3.5 equivalents of TTMSS, the desired product **2a** could be isolated in 91% ee with 66% yield (entry 14). Control experiments indicated that the electricity, TTMSS, and catalyst are necessary to succeed in this transformation (entries 15 and 16). Replacement of α -chloro esters with α -bromoesters resulted in a low yield of the desired product, but good enantioselectivity (91%) was obtained (Supplementary Table 8).

Substrate scope

With suitable reaction conditions in hand, the substrate scope was investigated to probe the generality and to identify the limitations of

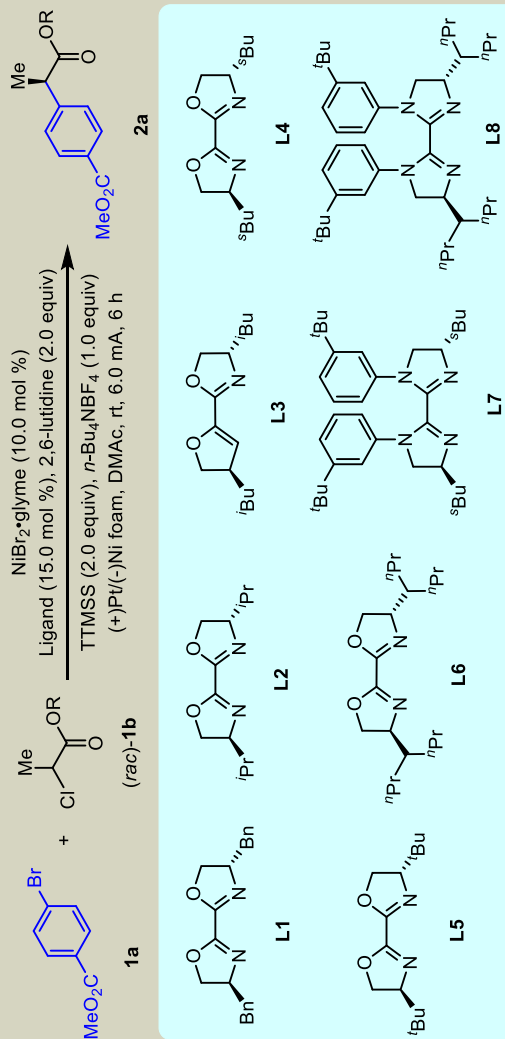
Table 1 | Reaction optimization and control studies^a

Entry ^a	Ligand	R	Yield (%)	ee (%)
1	di-Bubpy	Et	91 (90) ^b	-
2	L1	Et	10	44
3	L2	Et	20	72
4	L3	Et	37	46
5	L4	Et	25	77
6	L5	Et	<5	-
7	L4	PMP	20	67
8	L4	Pr	15	76
9	L4	tBu	15	77
10	L4	2,3,3-Trimethylbut-2-yl	10	84
11	L6	2,3,3-Trimethylbut-2-yl	11	89
12	L7	2,3,3-Trimethylbut-2-yl	30	90
13	L8	2,3,3-Trimethylbut-2-yl	25	84
14	L7	2,3,3-Trimethylbut-2-yl	66 ^c	91
15	no electric current or TTMS	2,3,3-Trimethylbut-2-yl	<5	-
16	No NiBr ₂ glyme or L7	2,3,3-Trimethylbut-2-yl	<5	-

^aReaction conditions: **1a** (0.2 mmol), (rac)-**1b** (2.0 equiv), NiBr₂glyme (10.0 mol%), 2,6-lutidine (2.0 equiv), TTMS (2.0 equiv), n-Bu₄NBF₄ (1.0 equiv), and DMAc (2.0 mL) at, in an undivided cell subjected to 6.0 mA of current for 6.0 h using platinum anode (1.0 cm × 1.0 cm) and Ni foam cathode (2.0 × 3.0 cm²), argon. The yield was determined by ¹H NMR using CH₂Br₂ as an internal standard. Enantioselectivities were determined by chiral HPLC analysis.

^bIsolated yield in parentheses.

^cLutidine (3.0 equiv), Tris(trimethylsilyl)silane (3.5 equiv), U_{cell} = 2.9 V for 6.0 h.



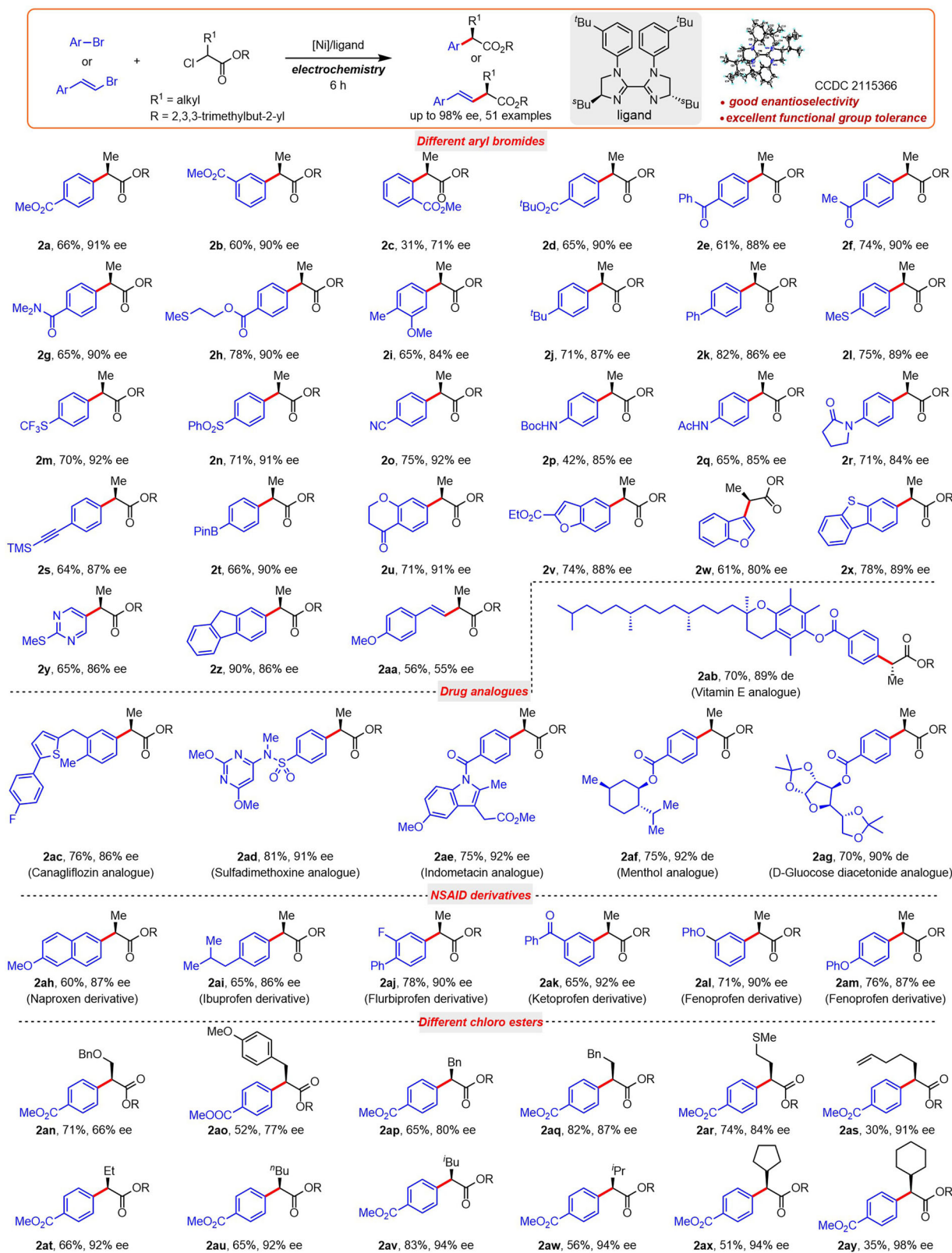


Fig. 2 | Evaluation of substrate scope. Yield of isolated products unless otherwise indicated. The reaction was carried out in an undivided cell with **1a** (0.2 mmol), (*rac*)-**1b** (2.0 equiv), $\text{NiBr}_2 \cdot \text{glyme}$ (10.0 mol%), **L7** (15.0 mol%), DMAc (0.1 M), *n*-Bu₄NBF₄ (1.0 equiv), TTMSS (3.5 equiv), 2,6-lutidine (3.0 equiv), platinum anode

(1.0 cm × 1.0 cm) and Ni foam cathode (2.0 cm × 3.0 cm), constant potential ($U_{\text{cell}} = 2.9 \text{ V}$, 6.0 h for 0.2 mmol scale), rt. Enantioselectivities were determined by chiral HPLC analysis. TTMSS stands for Tris(trimethylsilyl)silane.

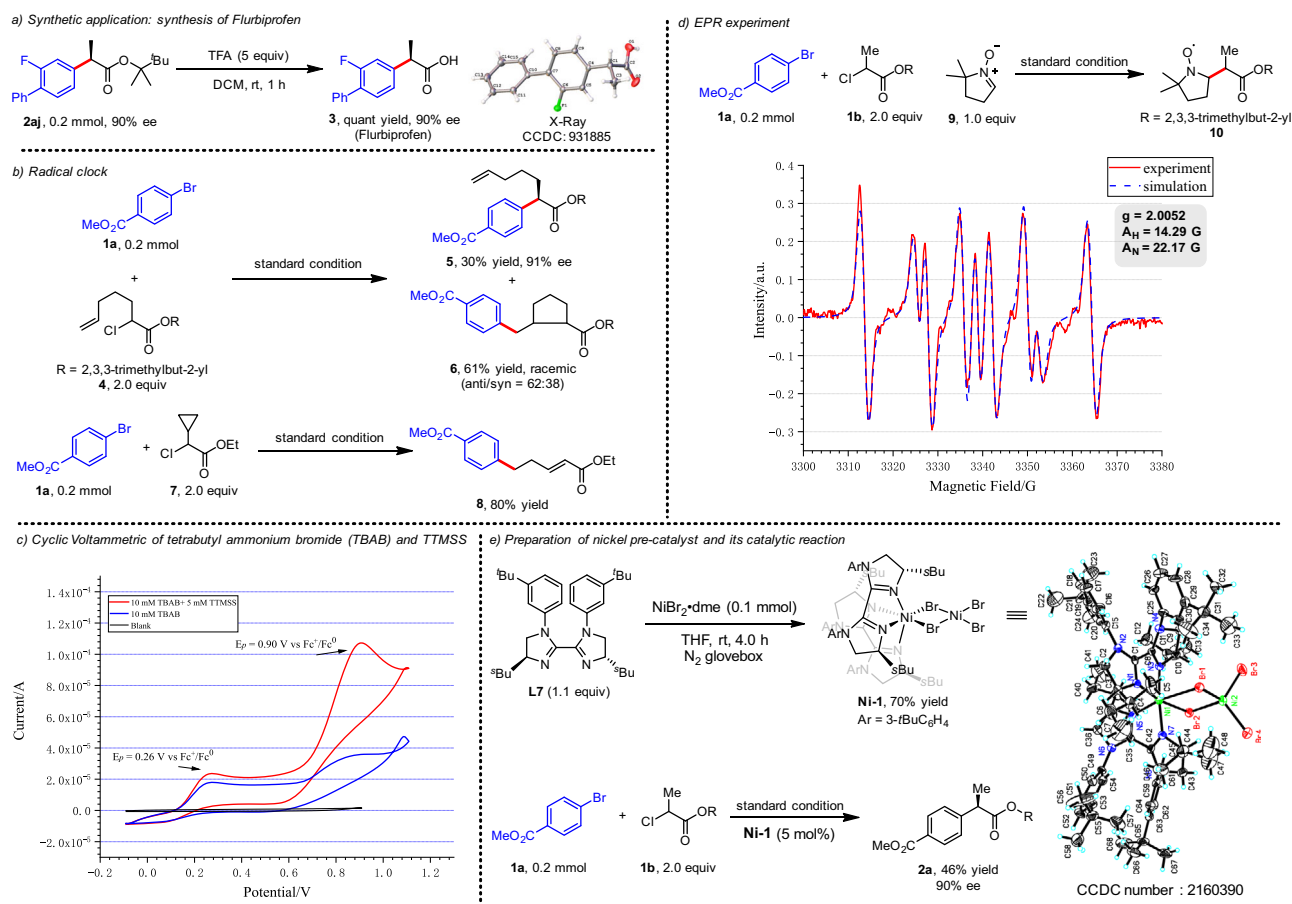


Fig. 3 | Synthetic application and mechanistic studies. a Synthetic application: synthesis of flurbiprofen. **b** Radical clock. **c** Cyclic voltammetric of tetra-butyl ammonium bromide (TBAB) and TTMSS. **d** EPR experiment. **e** Preparation of nickel precatalyst and its catalytic reaction.

these Ni-catalyzed asymmetric electrochemical arylations (as shown in Fig. 2). The position of substituents has a strong influence on both yield and enantioselectivity of the coupling products (**2a–2c**). Excellent functional group tolerance was observed, including ester (**2d**), ketone (**2e**, **2f**), amide (**2g**), methylthio (**2h**, **2i**), ether (**2i**), alkyl (**2j**), as well as aryl (**2k**) substituents. Aryl bromides with electron-withdrawing groups (**2m–2r**) exhibited good enantioselectivity (84–92%). It is noteworthy that the trimethylsilyl and boronate ester were also both well accommodated under electrochemical conditions, affording the products **2s** and **2t** in 64 and 66% yield with 87 and 90% ee, respectively. Heterocycles such as chromanone, benzofuran, benzothio-phenone, and pyrimidine proved to be good coupling partners, affording the corresponding products **2u–2y** in good yield and 86–91% ee. For other evaluated heteroaryl bromides, low conversion of 3-bromoquinoline, 3-bromopyridine, 6-bromobenzo[d]oxazole, and 2-bromo-1H-imidazole were observed (Supplementary Table 8). Excellent yield and good enantioselectivity were observed when 2-bromofluorene was employed (**2z**). An alkenyl bromide afforded moderate yield and diminished enantioselectivity of the corresponding product **2aa**. Unfortunately, aryl iodide, chloride, and alkenyl triflates were unsuccessful under present reaction conditions (see Supplementary Table 8 for details).

To illustrate the synthetic utility of our protocol, we applied it to the preparation of α -aryl ester derivatives of analogs of several known medicines, including those of canagliflozin, sulfadimethoxine, indomethacin, (–)-menthol, and D-glucose diacetate, affording the corresponding products **2ab–2ag** in 70–81% yield and 86–92% enantioselectivity. Furthermore, six well-known NSAID derivatives (**2ah–2am**) were readily synthesized using our method. These results

demonstrate the breadth of opportunity available for modern applications in drug discovery and agrochemical synthesis.

The influence of the α -alkyl substituent of the α -chloro ester reactant was also probed. Ether-bearing esters afforded either lower enantioselectivity or yield (**2an** and **2ao**, respectively). A benzyl substituent afforded attenuated enantioselectivity (**2ap**), whereas a homobenzyl substituent fared much better in terms of both yield and enantioselectivity (**2aq**). Methanethio fared marginally better than benzyl in terms of both yield and enantioselectivity (**2ar**). Enantioselectivities ranged from 91–98% for non-arene-bearing hydrocarbon substituents, though yields varied widely (**2as–2ay**).

Discussion

Flurbiprofen was readily prepared by quantitative hydrolysis of **2aj**, and was found to have (*R*) configuration by X-ray analysis (Fig. 3a). To gain insight into the mechanism of this electrochemical cross-coupling, we reacted **1a** with radical clocks **4** and **7**. Cyclized product **6** was obtained from **4** as a racemic mixture of diastereomers (61% yield, *trans:cis* = 62:38) (Fig. 3b). When cyclopropyl-containing **7** was employed, ring-opened product **8** was formed with 80% yield. These results suggest that this nickel-catalyzed cross-coupling process likely involves a radical pathway.

Next, we probed the electrochemical cross-coupling reaction mechanism via cyclic voltammetric analyses (Fig. 3c). A 0.1 M solution of TBAB in DMAC, exhibits oxidation peaks at 0.26 and 0.90 V versus Fc^+/Fc^0 (see Supplementary Fig. 2 for details). An increase in the second oxidation peak was observed after TTMSS (5 mM) was added. This result indicates that the bromide anion is converted to an electrophilic bromine radical following oxidation; bromine radicals are known to

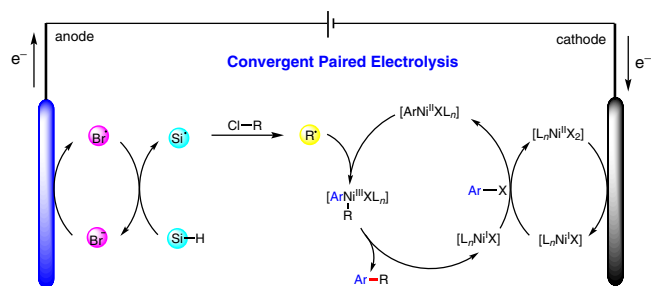


Fig. 4 | Plausible mechanism. The electrophilic alkyl radical from the α -carbonyl chloride is formed via XAT and HAT processes in the anode. Cathodic reduction of $\text{Ni}^{\text{II}}\text{X}_2\text{L}_n$ species leads to $\text{Ni}^{\text{I}}\text{XL}_n$ species, which undergoes the oxidative addition of aryl halides. The capture of the alkyl radical by $\text{Ni}^{\text{I}}\text{XL}_n$ species delivers an (alkyl)(aryl) $\text{Ni}^{\text{III}}\text{XL}_n$ species, then rapid reductive elimination yields product **2** and regenerates the Ni species.

rapidly abstract a hydrogen atom from the silane. The silyl radical can then rapidly abstract a chlorine atom from the activated α -carbonyl chloride to generate an electrophilic alkyl radical species^{66,67}. The alkyl radical was trapped by DMPO (5,5-dimethyl-1-pyrroline *N*-oxide) and the resulting more stable radical **10** was detected by EPR (electron paramagnetic resonance, Fig. 3d). Finally, nickel precatalyst (**Ni-1**) was synthesized by reacting $\text{NiBr}_2\cdot\text{dme}$ and chiral BiLM ligand **L7** at room temperature for 4 h, and its structure was verified by X-ray analysis (Fig. 3e). Interestingly, hexa-coordinated and tetra-coordinated nickel species constitute this binuclear nickel complex **Ni-1**. We performed the reaction with **Ni-1** as the catalyst, the desired product **2a** was obtained in 46% yield with 90% ee (Fig. 2e). Although **Ni-1** provides good reactivity and enantioselectivity in this transformation, the 1:1 coordination of nickel and BiLM as catalytic activity species cannot be ruled out. Based on the mechanistic experiments above, and the related studies by Diao^{68,69,85,86}, we propose the putative mechanism shown in Fig. 4. Initially, the anode oxidizes the bromide anion to a bromine radical, which can rapidly abstract a hydrogen atom from the silane. The resulting silyl radical can abstract the chlorine atom from the α -carbonyl chloride to generate an electrophilic alkyl radical species. The $\text{Ni}^{\text{II}}\text{X}_2\text{L}_n$ species is reduced to a $\text{Ni}^{\text{I}}\text{XL}_n$ species by cathodic reduction. Then, following oxidative addition in the presence of another $\text{Ni}^{\text{I}}\text{XL}_n$ species, an $\text{ArNi}^{\text{III}}\text{XL}_n$ intermediate and $\text{Ni}^{\text{II}}\text{X}_2\text{L}_n$ are generated^{68,69}. Oxidative capture of an α -acyl radical could then deliver an (alkyl)(aryl) $\text{Ni}^{\text{III}}\text{XL}_n$ species, which then undergoes rapid reductive elimination to form the $\text{C}(\text{sp}^2)\text{-C}(\text{sp}^3)$ bond of **2** and regenerate the Ni species. However, a $\text{Ni}^{\text{0}}/\text{Ni}^{\text{I}}/\text{Ni}^{\text{II}}/\text{Ni}^{\text{III}}$ catalysis sequence (rather than the aforementioned $\text{Ni}^{\text{I}}/\text{Ni}^{\text{II}}/\text{Ni}^{\text{III}}$ sequence) cannot be ruled out at this stage.

In summary, we develop a paired electrolysis-enabled Ni-catalyzed enantioselective reductive cross-coupling of aryl bromides and α -chloro esters under mild reaction conditions, affording enantio-enriched α -aryl esters with good yields. Additionally, various non-steroidal anti-inflammatory drug (NSAID) derivatives can be efficiently synthesized, and numerous drug analogs can be diversified through these asymmetric electrochemical reductive couplings. In this electrochemical process, alkyl radicals are generated from alkyl halides through a sequential electron transfer process involving anodic oxidation, while at the same time, the nickel catalyst is reduced to a lower oxidation state via cathodic reduction. Preliminary mechanistic experiments strongly support the synergistic involvement of anodic and cathodic redox events.

Methods

General procedure for the electrolysis

In a nitrogen-filled glove box, an over-dried 10 mL hydrogenation tube charged with a stir bar, $\text{NiBr}_2\cdot\text{glyme}$ (10.0 mol%, 6.2 mg), **L** (15.0 mol%,

16.0 mg), TBABF_4 (62.0 mg, 0.2 mmol) and DMAc (1.0 mL) were added to the electrochemical cell and the mixture was stirred for over 20 min. Then aryl bromide (0.2 mmol), 2,3,3-trimethylbutan-2-yl-2-chloropropanoate (90.0 mg, 0.4 mmol), 2,6-lutidine (62.0 mg, 0.6 mmol), TTMSS (175.0 mg, 0.70 mmol), and DMAc (1.0 mL) were added to the electrochemical cell. The tube was installed with Ni foam (2.0 cm \times 3.0 cm) as the cathode and Pt (1.0 cm \times 1.0 cm) as the anode. The seal tube was sealed and removed from the glove box. The reaction mixture was electrolyzed under a constant current of 2.9 V until the complete consumption of the starting materials was judged by TLC (about 6 h). After the reaction, the aqueous layer was extracted with EtOAc (3 x equal volume) and the combined organics were washed with sat. brine (4 x equal volume), dried over MgSO_4 , filtered and concentrated in vacuo. The crude product was purified by column chromatography to furnish the desired product.

More experimental procedures and a photographic guide for Ni-catalyzed enantioselective electrochemical reductive cross-couplings are provided in the Supplementary Information.

Data availability

The X-ray crystallographic coordinates for structures reported in this article have been deposited at the Cambridge Crystallographic Data Center (CCDC), under deposition number CCDC 2115366 (**L7**), CCDC 931885 (**3**), and CCDC 2160390 (**Ni-1**). The data can be obtained free of charge from the Cambridge Crystallographic Data Center [http://www.ccdc.cam.ac.uk/data_request/cif]. The data supporting the findings of this study are available within the article and its Supplementary Information files. Any further relevant data were available from the authors on request.

References

- Lin, Q., Li, L. & Luo, S. Asymmetric electrochemical catalysis. *Chem. Eur. J.* **25**, 10033–10044 (2019).
- Ghosh, M., Shinde, V. S. & Rueping, M. A review of asymmetric synthetic organic electrochemistry and electrocatalysis: concepts, applications, recent developments and future directions. *Beilstein J. Org. Chem.* **15**, 2710–2746 (2019).
- Yamamoto, K., Kuriyama, M. & Onomura, O. Anodic oxidation for the stereoselective synthesis of heterocycles. *Acc. Chem. Res.* **53**, 105–120 (2020).
- Chang, X., Zhang, Q. & Guo, C. Asymmetric electrochemical transformations. *Angew. Chem. Int. Ed.* **59**, 12612–12622 (2020).
- Wang, X., Xu, X., Wang, Z., Fang, P. & Mei, T. Advances in asymmetric organotransition metal-catalyzed electrochemistry. *Chin. J. Org. Chem.* **40**, 3738–3747 (2020).
- Jensen, K. L., Franke, P. T., Nielsen, L. T., Daasbjerg, K. & Jørgensen, K. A. Anodic oxidation and organocatalysis: direct regio- and stereoselective access to meta-substituted anilines by α -arylation of aldehydes. *Angew. Chem. Int. Ed.* **49**, 129–133 (2010).
- Fu, N., Li, L., Yang, Q. & Luo, S. Catalytic asymmetric electrochemical oxidative coupling of tertiary amines with simple ketones. *Org. Lett.* **19**, 2122–2125 (2017).
- Lu, F.-Y. et al. Highly enantioselective electrosynthesis of C2-quaternary indolin-3-ones. *Chem. Commun.* **56**, 623–626 (2020).
- Li, L., Li, Y., Fu, N., Zhang, L. & Luo, S. Catalytic asymmetric electrochemical α -arylation of cyclic β -ketocarboxyls with anodic benzyne intermediates. *Angew. Chem. Int. Ed.* **59**, 14347–14351 (2020).
- Chang, X., Zhang, J., Zhang, Q. & Guo, C. Merging electrosynthesis and bifunctional squaramide catalysis in the asymmetric difluoroacetylation reactions. *Angew. Chem. Int. Ed.* **59**, 18500–18504 (2020).
- Wang, Z.-H. et al. TEMPO-enabled electrochemical enantioselective oxidative coupling of secondary acyclic amines with ketones. *J. Am. Chem. Soc.* **143**, 15599–15605 (2021).

12. Torii, S., Liu, P. & Tanaka, H. Electrochemical Os-catalyzed asymmetric dihydroxylation of olefins with Sharpless' ligand. *Chem. Lett.* **24**, 319–320 (1995).
13. Durandetti, M., Périchon, J. & Nédélec, J.-Y. Asymmetric induction in the electrochemical cross-coupling of aryl halides with α -chloropropionic acid derivatives catalyzed by nickel complexes. *J. Org. Chem.* **62**, 7914–7915 (1997).
14. Franco, D., Riahi, A., Hénin, F., Muzart, J. & Duñach, E. Electrochemical reduction of a racemic allyl β -keto ester catalyzed by nickel complexes: asymmetric induction. *Eur. J. Org. Chem.* **2002**, 2257–2259 (2002).
15. Chen, B.-L. et al. Asymmetric electrocarboxylation of 1-phenylethyl chloride catalyzed by electrogenerated chiral [Co(salen)]-complex. *Electrochem. Commun.* **42**, 55–59 (2014).
16. Jiao, K.-J. et al. Palladium-catalyzed reductive electrocarboxylation of allyl esters with carbon dioxide. *Org. Chem. Front.* **5**, 2244–2248 (2018).
17. Fu, N. et al. New bisoxazoline ligands enable enantioselective electrocatalytic cyanofunctionalization of vinylarenes. *J. Am. Chem. Soc.* **141**, 14480–14485 (2019).
18. DeLano, T. J. & Reisman, S. E. Enantioselective electroreductive coupling of alkenyl and benzyl halides via nickel catalysis. *ACS Catal.* **9**, 6751–6754 (2019).
19. Zhang, Q., Chang, X. & Guo, C. Asymmetric Lewis acid catalyzed electrochemical alkylation. *Angew. Chem. Int. Ed.* **58**, 6999–7003 (2019).
20. Dhawa, U. et al. Enantioselective pallada-electrocatalyzed C–H activation by transient directing groups: expedient access to helicenes. *Angew. Chem. Int. Ed.* **59**, 13451–13457 (2020).
21. Qiu, H. et al. Enantioselective Ni-catalyzed electrochemical synthesis of biaryl atropisomers. *J. Am. Chem. Soc.* **142**, 9872–9878 (2020).
22. Robinson, S. G., Wu, X., Jiang, B., Sigman, M. S. & Lin, S. Mechanistic studies inform design of improved Ti(salen) catalysts for enantioselective [3 + 2] cycloaddition. *J. Am. Chem. Soc.* **142**, 18471–18482 (2020).
23. Song, L. et al. Dual electrocatalysis enables enantioselective hydrocyanation of conjugated alkenes. *Nat. Chem.* **12**, 747–754 (2020).
24. Li, W., Nonaka, T. & Chou, T.-C. Paired electrosynthesis of organic compounds. *Electrochemistry* **67**, 4–10 (1999).
25. Pletcher, D., Green, R. A. & Brown, R. C. D. Flow electrolysis cells for the synthetic organic chemistry laboratory. *Chem. Rev.* **118**, 4573–4591 (2018).
26. Hilt, G. Basic strategies and types of applications in organic electrochemistry. *ChemElectroChem* **7**, 395–405 (2020).
27. Sbei, N., Hardwick, T. & Ahmed, N. Green chemistry: electrochemical organic transformations via paired electrolysis. *ACS Sustain. Chem. Eng.* **9**, 6148–6169 (2021).
28. Zhang, W., Hong, N., Song, L. & Fu, N. Reaching the full potential of electroorganic synthesis by paired electrolysis. *Chem. Rec.* **21**, 2574–2584 (2021).
29. Dong, X., Roeckl, J. L., Waldvogel, S. R. & Morandi, B. Merging shuttle reactions and paired electrolysis for reversible vicinal dihalogenations. *Science* **371**, 507–514 (2021).
30. Zhang, S. et al. Electrochemical arylation of aldehydes, ketones, and alcohols: from cathodic reduction to convergent paired electrolysis. *Angew. Chem. Int. Ed.* **60**, 7275–7282 (2021).
31. You, S. et al. Paired electrolysis enabled annulation for the quinolyl-modification of bioactive molecules. *Chem. Sci.* **13**, 2310–2316 (2022).
32. Zhang, S. & Findlater, M. Progress in convergent paired electrolysis. *Chem. Eur. J.* **28**, e202201152 (2022).
33. Li, C. et al. Electrochemically enabled, nickel-catalyzed amination. *Angew. Chem. Int. Ed.* **56**, 13088–13093 (2017).
34. Zhang, L. & Hu, X. Nickel catalysis enables convergent paired electrolysis for direct arylation of benzylic C–H bonds. *Chem. Sci.* **11**, 10786–10791 (2020).
35. Liang, Y. et al. Electrochemically induced nickel catalysis for oxygenation reactions with water. *Nat. Catal.* **4**, 116–123 (2021).
36. Luo, Z. et al. One-pot synthesis of tertiary amides from organic trichlorides through oxygen atom incorporation from air by convergent paired electrolysis. *J. Org. Chem.* **86**, 5983–5990 (2021).
37. Li, Z. et al. Electrochemically enabled, nickel-catalyzed dehydroxylative cross-coupling of alcohols with aryl halides. *J. Am. Chem. Soc.* **143**, 3536–3543 (2021).
38. Wei, L. et al. Esterification of carboxylic acids with aryl halides via the merger of paired electrolysis and nickel catalysis. *J. Org. Chem.* **86**, 15906–15913 (2021).
39. Luo, J., Hu, B., Wu, W., Hu, M. & Liu, T. L. Nickel-catalyzed electrochemical C(sp³)-C(sp²) cross-coupling reactions of benzyl trifluoroborate and organic halides. *Angew. Chem. Int. Ed.* **60**, 6107–6116 (2021).
40. Ma, Y. et al. Direct arylation of α -amino C(sp³)-H bonds by convergent paired electrolysis. *Angew. Chem. Int. Ed.* **58**, 16548–16552 (2019).
41. Mo, Y. et al. Microfluidic electrochemistry for single-electron transfer redox-neutral reactions. *Science* **368**, 1352–1357 (2020).
42. Yates, P. et al. A novel type of indole alkaloid. *J. Am. Chem. Soc.* **95**, 7842–7850 (1973).
43. Ito, T. et al. Three new resveratrol oligomers from the stem bark of *Vatica pauciflora*. *J. Nat. Prod.* **67**, 932–937 (2004).
44. Landoni, M. F. & Soraci, A. Pharmacology of chiral compounds 2-arylpropionic acid derivatives. *Curr. Drug Metab.* **2**, 37–51 (2001).
45. Hao, Y.-J., Hu, X.-S., Zhou, Y., Zhou, J. & Yu, J.-S. Catalytic enantioselective α -arylation of carbonyl enolates and related compounds. *ACS Catal.* **10**, 955–993 (2020).
46. Hamada, T., Chieffi, A., Åhman, J. & Buchwald, S. L. An improved catalyst for the asymmetric arylation of ketone enolates. *J. Am. Chem. Soc.* **124**, 1261–1268 (2002).
47. Xie, X., Chen, Y. & Ma, D. Enantioselective arylation of 2-methylacetoacetates catalyzed by CuI/trans-4-hydroxy-L-proline at low reaction temperatures. *J. Am. Chem. Soc.* **128**, 16050–16051 (2006).
48. Liao, X., Weng, Z. & Hartwig, J. F. Enantioselective α -arylation of ketones with aryl triflates catalyzed by difluorophos complexes of palladium and nickel. *J. Am. Chem. Soc.* **130**, 195–200 (2008).
49. Guo, J. et al. Chiral scandium(III)-catalyzed enantioselective α -arylation of nonprotected 3-substituted oxindoles with diaryliodonium salts. *Angew. Chem. Int. Ed.* **52**, 10245–10249 (2013).
50. Ghosh, A., Walker, J. A., Ellern, A. & Stanley, L. M. Coupling catalytic alkene hydroacylation and α -arylation: enantioselective synthesis of heterocyclic ketones with α -chiral quaternary stereocenters. *ACS Catal.* **6**, 2673–2680 (2016).
51. Rao, X. et al. Efficient synthesis of (-)-corynoline by enantioselective palladium-catalyzed α -arylation with sterically hindered substrates. *Angew. Chem. Int. Ed.* **57**, 12328–12332 (2018).
52. Willis, M. C., Powell, L. H. W., Claverie, C. K. & Watson, S. J. Enantioselective Suzuki reactions: catalytic asymmetric synthesis of compounds containing quaternary carbon centers. *Angew. Chem. Int. Ed.* **43**, 1249–1251 (2004).
53. Eno, M. S., Lu, A. & Morken, J. P. Nickel-catalyzed asymmetric Kumada cross-coupling of symmetric cyclic sulfates. *J. Am. Chem. Soc.* **138**, 7824–7827 (2016).
54. Schmidt, J., Choi, J., Liu, A. T., Slusarczyk, M. & Fu, G. C. A general, modular method for the catalytic asymmetric synthesis of alkylboronate esters. *Science* **354**, 1265–1269 (2016).
55. Schafer, P., Palacin, T., Sidera, M. & Fletcher, S. P. Asymmetric Suzuki-Miyaura coupling of heterocycles via rhodium-catalysed allylic arylation of racemates. *Nat. Commun.* **8**, 15762–15769 (2017).

56. Varenikov, A. & Gandelman, M. Synthesis of chiral α -trifluoromethyl alcohols and ethers via enantioselective Hiyama cross-couplings of bisfunctionalized electrophiles. *Nat. Commun.* **9**, 3566–3572 (2018).
57. Guan, H., Zhang, Q., Walsh, P. J. & Mao, J. Nickel/photoredox-catalyzed asymmetric reductive cross-coupling of racemic α -chloro esters with aryl iodides. *Angew. Chem. Int. Ed.* **59**, 5172–5177 (2020).
58. DeLano, T. J. et al. Nickel-catalyzed asymmetric reductive cross coupling of α -chloroesters with (hetero)aryl iodides. *Chem. Sci.* **12**, 7758–7762 (2021).
59. Jiao, K.-J., Xing, Y.-K., Yang, Q.-L., Qiu, H. & Mei, T.-S. Site-selective C–H functionalization via synergistic use of electrochemistry and transition metal catalysis. *Acc. Chem. Res.* **53**, 300–310 (2020).
60. Ma, C. et al. Recent advances in organic electrocatalysis employing transition metal complexes as electrocatalysts. *Sci. Bull.* **66**, 2412–2429 (2021).
61. Yu, L., Jin, X. & Chen, G. Z. A comparative study of anodic oxidation of bromide and chloride ions on platinum electrodes in 1-butyl-3-methylimidazolium hexafluorophosphate. *J. Electroanal. Chem.* **688**, 371–378 (2013).
62. Yang, X. et al. Copper-catalyzed electrochemical selective bromination of 8-aminoquinoline amide using NH_4Br as the brominating reagent. *J. Org. Chem.* **85**, 3497–3507 (2020).
63. Yang, Q.-L. et al. Palladium-catalyzed electrochemical C–H bromination using NH_4Br as the brominating reagent. *Org. Lett.* **21**, 2645–2649 (2019).
64. Chatgililoglu, C. Organosilanes as radical-based reducing agents in synthesis. *Acc. Chem. Res.* **25**, 188–194 (1992).
65. Chatgililoglu, C., Ferreri, C., Landais, Y. & Timokhin, V. I. Thirty years of $(\text{TMS})_3\text{SiH}$: a milestone in radical-based synthetic chemistry. *Chem. Rev.* **118**, 6516–6572 (2018).
66. Chen, T. Q. & MacMillan, D. W. C. A metallaphotoredox strategy for the cross-electrophile coupling of α -chloro carbonyls with aryl halides. *Angew. Chem. Int. Ed.* **58**, 14584–14588 (2019).
67. Zhang, P., “Chip” Le, C. & MacMillan, D. W. C. Silyl radical activation of alkyl halides in metallaphotoredox catalysis: a unique pathway for cross-electrophile coupling. *J. Am. Chem. Soc.* **138**, 8084–8087 (2016).
68. Lin, Q. & Diao, T. Mechanism of Ni-catalyzed reductive 1,2-dicarbofunctionalization of alkenes. *J. Am. Chem. Soc.* **141**, 17937–17948 (2019).
69. Ju, L. et al. Reactivity of (bi-oxazoline)organonickel complexes and revision of a catalytic mechanism. *J. Am. Chem. Soc.* **143**, 14458–14463 (2021).
70. Ting, S. I., Williams, W. L. & Doyle, A. G. Oxidative addition of aryl halides to a Ni(I)-bipyridine complex. *J. Am. Chem. Soc.* **144**, 5575–5582 (2022).
71. Jin, M., Adak, L. & Nakamura, M. Iron-catalyzed enantioselective cross-coupling reactions of α -chloroesters with aryl Grignard reagents. *J. Am. Chem. Soc.* **137**, 7128–7134 (2015).
72. Poremba, K. E., Kadunce, N. T., Suzuki, N., Cherney, A. H. & Reisman, S. E. Nickel-catalyzed asymmetric reductive cross-coupling to access 1,1-diaryllkanes. *J. Am. Chem. Soc.* **139**, 5684–5687 (2017).
73. Woods, B. P., Orlandi, M., Huang, C.-Y., Sigman, M. H. & Doyle, A. G. Nickel-catalyzed enantioselective reductive cross-coupling of styrenyl aziridines. *J. Am. Chem. Soc.* **139**, 5688–5691 (2017).
74. Liu, H. & Du, D.-M. Recent advances in the synthesis of 2-imidazolines and their applications in homogeneous catalysis. *Adv. Synth. Catal.* **351**, 489–519 (2009).
75. Zhu, X., Niu, J., Zhao, X., Hao, X. & Song, M.-P. Synthesis of chiral bis(imidazoline) ligands with biphenyl backbone and their Application in the asymmetric cyclopropanation reaction. *Chin. J. Org. Chem.* **38**, 118–123 (2018).
76. Cheng, X., Lu, Z. & Lu, Z. Enantioselective benzylic C–H arylation via photoredox and nickel dual catalysis. *Nat. Commun.* **10**, 3549–3556 (2019).
77. He, Y., Yu, L. & Zhu, S. Enantio- and regioselective NiH-catalyzed reductive hydroarylation of vinylarenes with aryl iodides. *Angew. Chem. Int. Ed.* **59**, 21530–21534 (2020).
78. Zhu, W.-J., Gong, J.-F. & Song, M.-P. Synthesis of chiral bis(3-indolyl)-methanes bearing a trifluoromethylated all-carbon quaternary stereocenter via nickel-catalyzed asymmetric Friedel–Crafts alkylation reaction. *J. Org. Chem.* **85**, 9525–9537 (2020).
79. Cheng, X., Li, T., Liu, Y. & Lu, Z. Stereo- and enantioselective benzylic C–H alkenylation via photoredox/nickel dual catalysis. *ACS Catal.* **11**, 11059–11065 (2021).
80. Li, J., Yu, B. & Lu, Z. Chiral imidazoline ligands and their applications in metal-catalyzed asymmetric synthesis. *Chin. J. Chem.* **39**, 488–514 (2021).
81. Lau, S. H. et al. Ni/photoredox-catalyzed enantioselective cross-electrophile coupling of styrene oxides with aryl iodides. *J. Am. Chem. Soc.* **143**, 15873–15881 (2021).
82. He, Y., Song, H. & Zhu, S. L. NiH-catalyzed asymmetric hydroarylation of N-acyl enamines to chiral benzylamines. *Nat. Commun.* **12**, 638–644 (2021).
83. Wang, D. & Xu, T. A pivotal role of chloride ion on nickel-catalyzed enantioselective reductive cross-coupling to perfluoroalkylated boronate esters. *ACS Catal.* **11**, 12469–12475 (2021).
84. Zhou, P., Li, X., Wang, D. & Xu, T. Dual nickel- and photoredox-catalyzed reductive cross-coupling to access chiral trifluoromethylated alkanes. *Org. Lett.* **23**, 4683–4687 (2021).
85. Sicciani, J., Lin, Q. & Diao, T. Mechanisms of nickel-catalyzed coupling reactions and applications in alkene functionalization. *Acc. Chem. Res.* **53**, 906–919 (2020).
86. Dicciani, J. B. & Diao, T. Mechanisms of nickel-catalyzed cross-coupling reactions. *Trends Chem.* **1**, 830–844 (2019).

Acknowledgements

This work was financially supported by the National Key R&D Program of China (No. 2021YFA1500100), the NSF of China (Grants 21821002, 21772222, and 91956112), the S&TCSM of Shanghai (Grants 18JC1415600 and 20JC1417100), Bayer AG (Germany), and the fellowship of China Postdoctoral Science Foundation (2020M671274).

Author contributions

D.L., Z.-R.L., and Z.-H.W. designed and performed the experiments. T.-S.M. directed the project. C.M., S.H., and H.S. revised the manuscript. D.L., Z.-H.W., and T.-S.M. wrote the manuscript with input from all authors. All authors analyzed the results and commented on the manuscript.

Competing interests

The authors declare no competing interests.

Additional information

Supplementary information The online version contains supplementary material available at <https://doi.org/10.1038/s41467-022-35073-z>.

Correspondence and requests for materials should be addressed to Tian-Sheng Mei.

Peer review information *Nature Communications* thanks Yi Wang and the other, anonymous, reviewer for their contribution to the peer review of this work. Peer reviewer reports are available.

Reprints and permissions information is available at <http://www.nature.com/reprints>

Publisher's note Springer Nature remains neutral with regard to jurisdictional claims in published maps and institutional affiliations.

Open Access This article is licensed under a Creative Commons Attribution 4.0 International License, which permits use, sharing, adaptation, distribution and reproduction in any medium or format, as long as you give appropriate credit to the original author(s) and the source, provide a link to the Creative Commons license, and indicate if changes were made. The images or other third party material in this article are included in the article's Creative Commons license, unless indicated otherwise in a credit line to the material. If material is not included in the article's Creative Commons license and your intended use is not permitted by statutory regulation or exceeds the permitted use, you will need to obtain permission directly from the copyright holder. To view a copy of this license, visit <http://creativecommons.org/licenses/by/4.0/>.

© The Author(s) 2022